Environ. Sci. Technol. **2005**, *39,* 8466−8474

Degradation of Dye Pollutants by Immobilized Polyoxometalate with H_2O_2 under Visible-Light Irradiation

PENGXIANG LEI,[†] CHUNCHENG CHEN,[†] JUAN YANG,[†] WANHONG MA,[†] JINCAI ZHAO,*[,†] AND LING ZANG[‡]

Key Laboratory of Photochemistry, Center for Molecular Science, Institute of Chemistry, Chinese Academy of Sciences, Beijing 100080, China, and Department of Chemistry and Biochemistry, Southern Illinois University, Carbondale, Illinois 62901

A Keggin polyoxometalate (POM, i.e., $PW_{12}O_{40}^{3-}$) and its lacunary derivative are immobilized on an anionic exchange resin through electrostatic interaction at pH 4.6 in an aqueous dispersion. The resin-supported POM thus obtained catalyzes the efficient degradation of cationic dye pollutants in the presence of H_2O_2 under visible-light irradiation. To evaluate the photocatalytic system, degradation of a rhodamine B (RB) dye was investigated in detail using UV−visible spectroscopy, high performance liquid chromatography, and gas chromatography/mass spectrometry techniques to identify the intermediates and final products. Fluorescence lifetime measurements revealed the electron transfer from the visible-light-excited RB molecules to the POMs. Electron paramagnetic resonance measurements, investigation of the effects of •OH and •OOH scavengers on the photoreaction kinetics, and IR analysis indicated that de-ethylation of RB was due to •OOH radicals, but the decomposition of the conjugated xanthene structure was caused by the peroxo species formed by interaction of H_2O_2 with the lacunary POM loaded on the resin. A total organic carbon removal of ca. 22% was achieved, and the recycle experiment suggested excellent stability and reusability of the heterogeneous catalyst. On the basis of the experimental results, a photocatalytic mechanism is discussed.

Introduction

In recent years, polyoxometalates (POMs) have been a category of fast developing oxidative catalysts in organic synthesis and environmental remediation due to their diverse properties in molecular composition, redox potential, and solubility (*1*−*5*). The photochemistry and photocatalysis of POMs have aroused much interest, and it is recognized that POMs generally share the same photochemical characteristics of semiconductor photocatalysts such as TiO_2 (*5*, *6*). Upon UV irradiation, electrons are excited from the valence band to the conduction band of TiO_2, generating the electron−hole pairs in which the positive vacancies are powerful oxidants to destroy adsorbed organic substrates, while the conduction band electrons are trapped by molecular oxygen to form strong oxidative radicals such as •OOH and •OH that also cause the effective decomposition or even mineralization of organic substrates. Similarly, UV irradiation onto the POMs leads to a ligand-to-metal charge-transfer excited state with an oxidizing capacity over 2.5 V versus the normal hydrogen electrode (NHE) (*5*) by which most organic substrates could be easily oxidized. And at the same time, the reduced POMs are highly reductive. Therefore, the photodegradation of various organic pollutants (*7*−*10*) and the photoreduction of inorganic metal ions (*11*−*13*) mediated by POMs have been achieved.

With this understanding, most published works related to the photocatalysis of POMs are concentrated on UV irradiation, which only possesses less than 4% of the total solar energy reaching Earth's surface. Aiming at utilizing the inexpensive and inexhaustible solar energy, we and others (*14*−*17*) have investigated the photocatalytic behaviors of semiconductor catalysts in the degradation of dye pollutants under visible-light irradiation. In these cases, the mechanistic aspects differ greatly from those in the systems with UV irradiation. It involves electron injection from the photoexcited dye pollutants to the conduction band of TiO_2, then the conduction band electron reacts with molecular oxygen to form active oxygen species, causing decomposition of the formed cationic dye radicals, but no valence band holes are involved. Similarly, ground-state POMs are also possible to act as electron relays by accepting electrons from organic donors (*18*) or organometallic compounds (*19*), but the rapid back electron transfer impedes the utilization of the charge-separated states. If the electrons trapped on the POMs could be removed effectively, then the reaction of the thus formed positive organic radicals could be realized. In a recent work, we have reported the photodegradation of a rhodamine B dye in an aerated homogeneous solution of a Keggin POM anion, namely, $SiW_{12}O_{40}^{4-}$, under visible-light irradiation, in which only the de-ethylation reaction but not the ring cleavage of the dye molecule took place, and almost no mineralization of the dye pollutants was detected (*20*).

Considering the high solubility of POMs in aqueous media, some research groups have put forward great efforts for the recovery and reuse of POM catalysts: immobilization of POMs on active carbon (*21*−*23*) and carbon fibers (*24*), impregnation of POMs on TiO_2 or silica gels (*25*−*27*), intercalation of POMs into anionic clays (*28*), and the combination of POMs with suitable counterions such as Cs^+ (*29*) or organic dendrimers (*30*) to obtain insoluble catalysts. Besides the easy recovery of the POM catalysts, some support materials seem to enhance the catalytic reactivity of the combined catalysts. For example, Ozer and Ferry (*8*) achieved more rapid photodegradation of 1,2-dichlorobenzene by loading POMs on NaY zeolite in aerated dispersions under UV irradiation than in homogeneous POM solution; Hill and co-workers (*31*) reported the more efficient oxidation of sulfides and aldehydes in dark reactions by immobilization of POMs on cationic silica nanoparticles. Moreover, the surface effects of supports on the reaction pathways of POMs have also been recognized. Choi et al. (*32*) reported that immobilization of POMs on an inactive silica surface greatly changed the distribution of products in the photodegradation of 4-chlorophenol under UV irradiation and ascribed the changes to the introduction of a solid support surface that changed the surface chemistry and pathway of POM-mediated reaction.

However, H_2O_2 has been widely used as a "green" oxidant in organic synthesis and environmental remediation because (i) it generates H_2O as a sole byproduct, (ii) it has a high

* Corresponding author fax: +86-10-8261-6495; e-mail: jczhao@iccas.ac.cn.

[†] Chinese Academy of Sciences.

[‡] Southern Illinois University.

10.1021/es050321g CCC: $30.25
Published on Web 10/01/2005

content of active oxygen species, and (iii) it has an oxidative potential prevailing to molecular oxygen (1.76 V vs 0.695 V). Many POMs have been developed as effective catalysts for activating H_2O_2 in selective oxidation of various organic substrates in dark thermal reactions (*3*, *4*, *33*−*35*). It is also reported (*36*) that some POMs can catalyze efficient bleaching of organic dyes with H_2O_2 in the dark at pH 10.0; however, no information about the mineralization of these dye pollutants was offered.

We report herein the immobilization of a Keggin polyoxometalate, $PW_{12}O_{40}^{3-}$, on an anionic exchange resin under certain pH conditions in aqueous dispersion. The as-prepared material is used as an efficient catalyst in the degradation of organic dye pollutants *with* H_2O_2 under visible-light irradiation, in which the resin support provides a microenvironment for the preassociation of the catalyst, substrate, and oxidant that greatly enhances the reactivity of POMs compared to the homogeneous system. A rhodamine B (RB) dye, with the molecular structure shown below, was used as a model to examine the photocatalytic behavior of the photocatalyst. UV−vis spectra and total organic carbon (TOC) measurements showed that partial mineralization of the dye pollutant was achieved along with slight content of de-ethylation on the xanthene ring in the RB structure, which was further confirmed by the intermediates and ring cleavage final products detected by high performance liquid chromatography (HPLC) and gas chromatography/mass spectrometry (GC/MS) measurements. These results are significantly different from those in the photodegradation of RB in the presence of O_2 (without H_2O_2) catalyzed by homogeneously dissolved POM ($SiW_{12}O_{40}^{4-}$) under visible-light irradiation (*20*). The catalyst was readily separable and could be reused without obvious loss of catalytic activity. IR, electron paramagnetic resonance (EPR), and fluorescence lifetime measurements were used to explore the mechanistic aspects of the photoreaction. On the basis of the experimental results, a photocatalytic mechanism under visible-light irradiation is discussed.

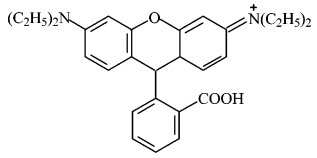

Experimental Section

Materials. α-$Na_3PW_{12}O_{40}\cdot xH_2O$ was purchased from Aldrich and used as received. α-$Na_4SiW_{12}O_{40}\cdot xH_2O$ and $Na_2WO_4\cdot 2H_2O$ were of analytic pure grade and purchased from the Beijing Chemical Reagent Company. Anionic exchange resin (D201 type) was kindly supplied by Nankai University. The target dye pollutants rhodamine B (RB), malachite green (MG), acridine orange (AO), sulforhodamine B (SRB), and orange II (OII) were obtained from Acros Chemical Company. The spin trapping reagent 5,5-dimethyl-pyrroline-oxide (DMPO) was obtained from Sigma. The deionized and doubly distilled water was used throughout this study, and the pH of the solutions was adjusted by diluted aqueous solutions of $HClO_4$ and NaOH.

Photoreactor and Light Source. A 500-W halogen lamp (Institute of Electric Light Source, Shanghai, China) used as the light source was positioned inside a cylindrical Pyrex vessel surrounded by a jacket with circulating water. A cutoff filter was used to remove wavelengths less than 450 nm completely and to ensure irradiation only by visible light.

Procedures and Analyses. The procedure for POM loading on the resin is as follows: The D201 resin was ground to powder and then treated with 1 M HCl and 1 M NaOH in sequence. After the resin was washed with pure water thoroughly and dried under vacuum, a definite amount of treated resin powder was suspended in water by magnetic stirring. Solutions of POM were introduced into the suspension to a given initial POM concentration, and the volume of the mixture was fixed to 50 mL. After being stirred magnetically for 2 h to allow the adsorption/desorption equilibration, the suspension was centrifuged, then dried in air, and the concentration of the POM remaining in the supernatant phase was determined spectroscopically.

Unless otherwise stated, all of the experiments were carried out in Pyrex vessels (60 mL) in aerated dispersions. At given time intervals, a 3-mL aliquot was drawn out, centrifuged, and analyzed immediately using a Lambda Bio 20 UV−visible spectrometer (Perkin-Elmer) to determine the concentration of the model pollutants. TOC determination of the supernatant liquid was performed on an Apollo 9000 analyzer (Tekmar Dohrmann). The de-ethylation intermediates of RB were determined by an HPLC method. The HPLC system consisted of a Dionex P580 pump, a UVD 340S Diode Array detector, and an intersil ODS-3 C_{18} reverse column (5 μm, 250 × 4.6 mm^2). GC/MS analyses were carried out on a Finnigan Trace DSQ Ultra instrument equipped with a DB-5 MS capillary column (30 m × 0.25 mm). The temperature program of the column was set as follows: at 60 °C, hold time = 1 min; from 60 to 250 °C, rate = 5 °C/min. The samples for GC/MS analyses were prepared as follows: After the catalyst particles were centrifuged, the aqueous solution was collected and evaporated to near dryness under reduced pressure; methanol (10 mL each time) was added and evaporated three times to remove water completely; finally, the remaining residue was dissolved in 0.5 mL of methanol. The EPR signals were detected on a Brucker model EPR 300E spectrometer equipped with a Quanta-Ray Nd:YAG laser (355 and 532 nm), and DMPO was used as the spin-trapper for the radicals. IR spectra were obtained on a DigiLab FTS 3500 Fourier transform IR spectrometer (Tekmar Dohrmann), and the samples were all supported on anhydrous KBr pellets. Fluorescence lifetimes were measured on a Horiba NAES-1100 time-resolved spectrofluorometer by the time-correlated single-photon counting method. To avoid the influence of scattering light, the exciting and receiving wavelengths were set at 500 and 590 nm, respectively.

Results and Discussion

Preparation and IR Spectra of the Photocatalyst. In this study, the D201 anionic exchange resin employed as a solid support for POMs is constructed of polystyrene with trimethylammonium groups at the side of the main chain. Since the negatively charged POMs can interact strongly with the alkylammonium groups through electrostatic interaction, POMs are loaded on the resin by mixing with the resin powder in an aqueous suspension. Therefore, the stability of the Keggin anions in aqueous solution should be taken into consideration. It is pointed out that Keggin anions are stable only under low pH conditions; for $PW_{12}O_{40}^{3-}$, this pH range is below 2.0, and it would decompose to some complicated structures or undergo complete decomposition depending on the pH beyond this range (*37*, *38*). However, as reported by Mizuno et al., the pH condition during POM catalyst preparation is related closely to its catalytic activity in a study of H_2O_2-based selective oxidation of organic substrates (*4a*). In the present procedure of $PW_{12}O_{40}^{3-}$ loading, pH conditions varying from 1.0 to 7.0 were tried by the addition of various amount of diluted $HClO_4$ solution, and finally pH 4.6 was adopted because the as-prepared catalyst showed the most efficient catalytic activity. The maximum loading amount of $PW_{12}O_{40}^{3-}$ on the D201 resin is ca. 5.1×10^{-4} mol g^{-1} resin.

Infrared measurement is a useful method in the characterization of POMs. Figure 1 showed the characteristic part (1200−400 cm^{-1} region) in the IR spectrum of the POM−

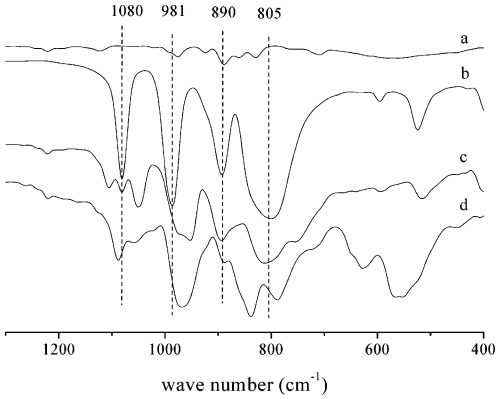

FIGURE 1. IR spectra of (a) resin, (b) POM ($Na_3PW_{12}O_{40}$), (c) POM−resin, and (d) POM−resin/H_2O_2.

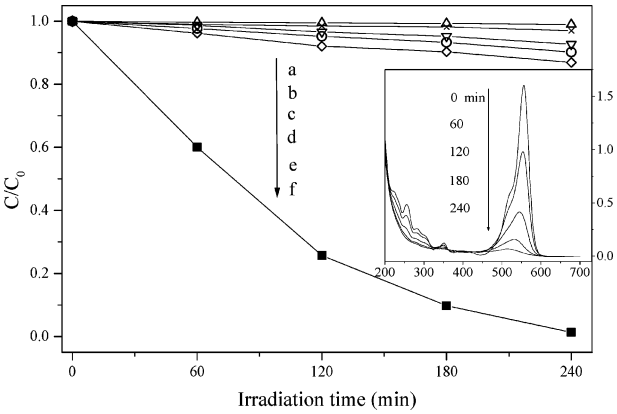

FIGURE 2. Kinetics of degradation of RB under different conditions: (a) POM−resin, H_2O_2, in the dark; (b) POM−resin, visible light; (c) H_2O_2, visible light; (d) resin, H_2O_2, visible light; (e) POM, H_2O_2, visible light; (f) POM−resin, H_2O_2, visible light. [RB] = 2.0×10^{-5} M; [H_2O_2] = 2.0×10^{-3} M; pH 2.5. Inset: UV−visible spectra changes of RB in the supernatant during irradiation for trace f.

resin (trace c) together with spectra of the resin (trace a) and the parent POM ($PW_{12}O_{40}^{3-}$, trace b) for comparison. Corresponding to the earlier reported data, the IR spectrum of $PW_{12}O_{40}^{3-}$ has four strong bands at 1080, 981, 890, and 805 cm^{-1}, which are designated to the stretching vibrations of P−O, W=O_t, W−O_c−W, and W−O_e−W, respectively (*39*). The IR spectrum of the bare resin (Figure 1, trace a) also showed some peaks, but when the same POM/resin ratio as in the POM−resin catalyst was employed in IR measurements, the vibrations of the resin were negligible compared to the strong bands of the POM. Some significant changes happened to the IR spectra of $PW_{12}O_{40}^{3-}$ by loading on the resin (trace c). Two new peaks emerged at ca. 1045 and 1110 cm^{-1}; as compared to the literature data for the characteristic P−O vibration of the lacunary anion $PW_{11}O_{39}^{7-}$, which is positioned at 1040 and 1085 cm^{-1} (*38*), shifts of 5 and 25 cm^{-1} were observed. The P−O vibration at 1080 cm^{-1} decreased but by no means disappeared, suggesting that there is still some complete $PW_{12}O_{40}^{3-}$ loaded on the resin surface. At the same time, the characteristic peak at 981 cm^{-1}, which is designated to the stretching vibration of terminal oxygen and the W atom (W=O_t), shifted to 968 cm^{-1}. However, vibrations of the W center with corner-sharing (O_c) and edge-sharing (O_e) oxygen atoms at 890 and 805 cm^{-1} seemed unchanged. All of the shifts in the IR spectra should be attributed to the effect of the resin support on the lacunary site and terminal oxygen atoms of the loaded POMs. The changes upon addition of H_2O_2 (trace d, Figure 1) will be discussed in the text below.

Photodegradation of Dye Pollutants. For the strong absorption in the visible-light region and excellent stability under various pH conditions, RB was chosen as the primary model dye pollutant to examine the photodegradation behaviors of the POM−resin catalyst in the presence of H_2O_2 under visible-light irradiation ($\lambda > 450$ nm). The degradation reactions were carried out after the establishment of the adsorption/desorption equilibrium by magnetic stirring for 30 min in the dark. After the equilibrium was established, about 20% of RB was adsorbed on the catalyst. The catalyst with a maximum POM loading, which exhibited the highest photoactivity for the degradation of dyes, was used in the following experiments, because the reactions with catalysts of 40%, 60%, and 80% of the maximum POM loading amount were much slower. Another Keggin ion, namely, $SiW_{12}O_{40}$,$^{4-}$ which was more stable in aqueous solution than $PW_{12}O_{40}^{3-}$ (*37*) and the metatungstate, WO_4^{2-}, were also loaded on the D201 resin and used as catalysts. However, they showed limited activity under the otherwise identical conditions.

The kinetics of the degradation of RB under different conditions is depicted in Figure 2. As shown in trace a, there was little degradation of RB observed in the presence of both catalyst and H_2O_2 in the dark, suggesting that visible-light irradiation is essential for the degradation of dye pollutants. Even under visible-light irradiation, RB was still difficult to degrade in the H_2O_2-only solution (trace c) or in dispersions with both resin and H_2O_2 (trace d) without POM in the system. The results suggest that the photosensitized auto-degradation of RB is a rather slow process, and no active sites are present on the bare resin support for H_2O_2 activation. Although it was reported that some POMs can activate H_2O_2 to bleach dye pollutants at pH 10.0 in the dark (*24*), only weak degradation of RB was observed (trace e) in homogeneous $PW_{12}O_{40}^{3-}$ solution in the presence of H_2O_2 at pH 2.5 even under visible-light irradiation. This is probably due to the fact that $PW_{12}O_{40}^{3-}$ is labile in dilute aqueous solution at pH 2.5, and H_2O_2 might accelerate the decomposition of $PW_{12}O_{40}^{3-}$ to some unknown species (*38*). A control experiment using WO_4^{2-} instead of $PW_{12}O_{40}^{3-}$ in a homogeneous solution also showed negligible activity under otherwise identical conditions. In the aerated dispersions without H_2O_2, the POM−resin catalyst exhibited limited activity for the degradation of RB under visible-light illumination (trace b) within the experimental time scale, while prolonged reaction time (20 h) resulted in the stepwise de-ethylation of RB as we have described in a previous work (*20*) in aerated homogeneous $SiW_{12}O_{40}^{4-}$ solution. However, as shown in trace f, upon addition of H_2O_2, the POM−resin catalyst presented considerable efficiency for the degradation of the RB dye under visible irradiation. During the photoreaction, the characteristic absorption band of RB at 551 nm diminished quickly, and a slight hypsochromic shift of the band was witnessed, due to the stepwise de-ethylation of *N*,*N*′-diethylammonium groups in the RB structure (*20*). The initial apparent rate constant was estimated to be 11.2 min^{-1}, following the first-order kinetic mode. It suggested the efficient decomposition of the conjugated xanthene ring in RB with a slight content of de-ethylation, which would be further examined by liquid chromatography (LC) and GC/MS measurements (see below). Before irradiation, the surface of the catalyst was red owing to the adsorption of RB; after exposure to visible light for 240 min, the supernatant phase was completely discolored, but the complete decolorization of the photocatalyst took some 120 min longer.

The photodegradation of some other dye pollutants by the POM−resin catalyst was also examined to verify the activity of the photocatalyst. Notably, the cationic dyes, such as MG and AO, could also undergo quick degradation in the presence of the photocatalyst and H_2O_2 under visible-light irradiation, but when anionic dyes such as SRB and OII were emlpoyed, hardly any degradation of these dye pollutants

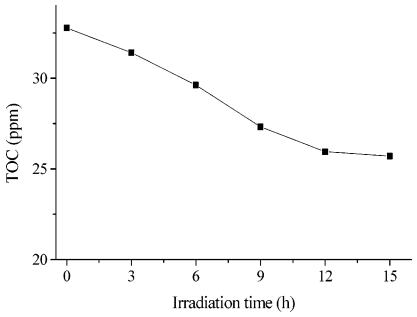

FIGURE 3. Temporal changes of TOC during the photodegradation of RB: catalyst loading, 5 mg; volume, 100 mL; [RB] = 1.0×10^{-4} M.

was observed. As stated above, the POMs are negatively charged, so they could interact with the positively charged cationic dyes and might repulse the anionic dye molecules. It is reasonable to infer that the interaction between the dye pollutants and POMs is a prerequisite for their photodegradation. Experiments with small molecules that have no absorption in the visible region were also investigated. Even in the case of those strongly interacting with the POM sites, such as benzyltrimethylammonium chloride (BTAC), no degradation was observed under visible irradiation, just like what happened in the case of RB in the dark (trace a, Figure 1), suggesting the importance of visible-light sensitization of the substrate.

From the kinetic study, one may conclude that visible light induced photosensitization of the dye, the oxidant H_2O_2 and the interaction between the dye molecules and the POM sites are all necessary for the efficient photodegradation of dye pollutants in the present system. Meanwhile, the resin support also plays an important role in the photocatalytic system, in a way that the homogeneuous system without resin support leads to a weak degradation of RB, while the resin-supported POMs can efficiently catalyze the degradation of RB under the otherwise identical conditions. And a reasonable explanation is that $PW_{12}O_{40}^{3-}$ is unstable under the reaction conditions, and the resin support prevents further decomposition of the POMs by the strong electrostatic interaction between POM and the alkylammonium groups on the resin.

TOC Measurement in the Degradation of RB. The mineralization degree of the RB dye was examined by the measurement of the decrease in TOC and the formation of CO_2 in the system. TOC changes during the degradation of RB under visible-light irradiation in the presence of the photocatalyst and H_2O_2 are depicted in Figure 3. To minimize experimental errors, the initial concentration of RB was promoted from 2.0×10^{-5} to 1.0×10^{-4} M, so the irradiation time needed for complete degradation RB also increased from 240 min to 12 h. During visible-light irradiation, the TOC value of the supernatant phase decreased gradually. The maximum TOC removal of RB reached ca. 22% at the point that the solution was discolored completely (12 h of irradiation). After that, the TOC value of the supernatant phase tended to keep constant. Consistent with the decrease in the TOC, the evolution of CO_2 (mineralization yield of RB into CO_2, ca. 24%) was also observed. From Figure 3, one could conclude that (1) partial mineralization of the dye pollutants did occur in the system and (2) the mineralization took place only before the reaction system had been completely discolored. Once the reaction system was discolored, there were no substrates to be excited by visible-light irradiation, which supplied energy for the photodegradation of RB, and the mineralization process ceased subsequently. In this regard, it was consistent with the dye/TiO_2 system in aerated dispersions under visible-light irradiation (*14*−*16*).

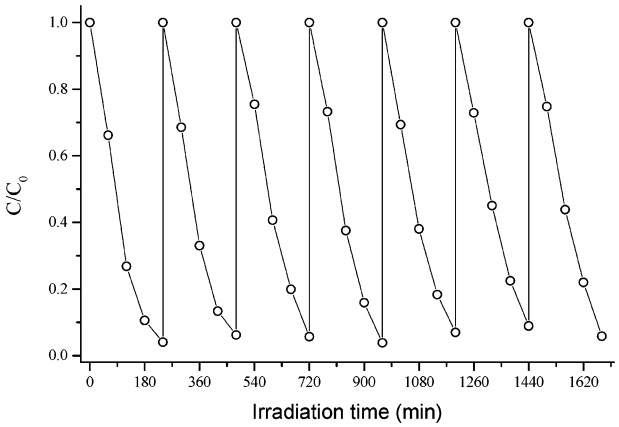

FIGURE 4. Catalyst recycle in repetitive degradation of RB (2.0×10^{-5} M/run) by H_2O_2 (2.0×10^{-3} M/run) in the presence of POM−resin (60 mg/L).

Recycle of the Catalyst. The stability and reusability of catalysts are very important issues for practical applications. Upon loading on the resin, the POMs could be readily recycled by simple centrifugation after reaction. The stability and reusability of the POM−resin were examined by repetitious use of the catalyst. As shown in Figure 4, after seven cycles for photodegradation of RB, the catalyst did not exhibit a significant loss of activity. In addition, there was no POM leaching from the resin support detected during the cycles. This suggested that the POM−resin catalyst is considerably stable during the photodegradation of the dyes. Some POMs, especially $PW_{12}O_{40}^{3-}$, have been used as catalyst precursors in homogeneous solution with concentrated hydrogen peroxide as an oxidant (*33*, *40*). In those cases, the original POMs decomposed to some certain structures to form the superoxo species, which accounted for oxidation of hydrocarbons. In contrast, the addition of H_2O_2 did not cause decomposition of POMs supported on the resin in the present system. This is most likely because (i) the concentration of H_2O_2 (10^{-3} M) used in the present system was much lower than that in those cases using commercially concentrated H_2O_2 (ca. 30 wt %, 10 M) and (ii) the positively charged ammonium groups on the resin might provide a function to stabilize to the supported POMs and prevent them from further decomposition.

Identification of the Intermediates and Final Products. Analyses of the reaction intermediates and final products are useful for evaluating the efficiency of catalytic systems and may reveal some details of the reaction process. Intermediates of RB during the photodegradation were monitored by HPLC equipped with a UV−visible diode array detector, and the results are illustrated in Figure 5. The RB dye used here is of 95% purity with a *N*,*N*-diethyl-*N*′-ethyl-rhodamine (DER) percentage of ca. 5%, which is consistent with HPLC analysis. During the photoreaction in the present system, three intermediates were observed, namely, DER, *N*-ethyl-*N*′-ethyl-rhodamine (EER), and *N*,*N*-diethyl-rhodamine (DR), corresponding to peaks b, c, and d in the inset of Figure 5, respectively, which resulted from losing one and/or two ethyl groups from the xanthene ring in the parent RB structure, as we have definitely determined with an LC/MS technique in a previous study (*20*). In Figure 5, with the quick disappearance of RB, the concentrations of DER, EER, and DR species increased slightly and then decreased with further visible irradiation. This proved that de-ethylation of RB did take place in the present system, but it was far from being the dominant process as what was observed in an aerated homogeneous $SiW_{12}O_{40}^{4-}$ system without H_2O_2 (*20*). Instead, decomposition of the conjugated chromophore structure of RB should be the major process. It was confirmed by the

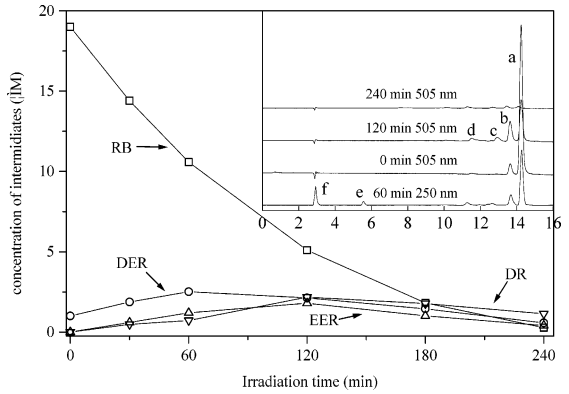

FIGURE 5. Variations in the distribution of the intermediates from the photodegradation of RB in the presence of POM−resin and H_2O_2. Inset: HPLC chromatograms of the intermediates recorded at 250 and 505 nm at different time intervals.

TABLE 1. Final Products of the Photodegradation of RB Detected by GC/MS[a]

retention time (min)	deleted product	relative amount
3.5	HCOOH	0.47
3.7	CH_3COOH	1.00
4.8	HOOCCOOH	0.89
6.8	$HOOCCH_2COOH$	0.76
9.6	$HOOCCH_2\ CH_2COOH$	0.53
17.2	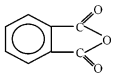	0.16
20.8	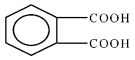	0.37

[a] Note that all of the acids except phthalic anhydride were detected in the form of methanolic esters because the samples were prepared in methanol.

emergence of a new peak (monitored in the UV region, $\lambda =$ 250 nm) with a retention time of ca. 5.5 min (peak e, inset of Figure 5) after the reaction initiated. The peak was supposed to represent some highly polar components that could not be separated by HPLC, and these components were most likely the small molecule intermediates resulting from the cleavage of the xanthene ring in RB structure.

To obtain more information about the highly polar and small molecular weight intermediates that could not be separated and identified by HPLC, the degradation products were analyzed further by a GC/MS technique. The major final products detected are listed in Table 1. They were mainly organic acids, such as formic acid, acetic acid, oxalic acid, succinic acid, and phthalic acid. Phthalic anhydride detected at a retention time of 17.2 min was probably formed from phthalic acid during the sample preparation. These GC/MS results provided solid evidence for the cleavage of the conjugated xanthene structure of both RB and the de-ethylated intermediates during the degradation reaction in the presence of POM/resin catalyst and H_2O_2, and it is significantly different with the photoreaction in an aerated homogeneous POM solution in which neither cleavage of the xanthene ring nor mineralization of the substrate was observed (*20*).

Fluorescence Lifetime Measurements of RB. The steady-state and time-resolved fluorescence analyses are usually used to investigate the excited-state characteristics and the photoinduced charge-transfer processes of the substrates. RB has strong fluorescence in dilute aqueous solution because of the conjugated xanthene ring in its molecular structure. However, the fluorescence of RB could be gradually quenched upon addition of POMs, due to the electron transfer from the excited dye to the POMs. To clarify the charge-transfer characteristics between the photoexcited RB dye and the catalyst in the absence/presence of H_2O_2, we performed the fluorescence lifetime analyses of RB under various conditions, and the results were summarized in Table 2.

TABLE 2. Fluorescence Lifetimes of RB in Different Systems

entry	reaction system	lifetime (ns)	percentage (%)
1	RB	$\tau = 1.5 \pm 0.1$	
2	RB/POM	$\tau = 1.2 \pm 0.1$	
3	RB/resin	$\tau = 6.0 \pm 0.3$	
4	RB/resin/H_2O_2	$\tau = 6.1 \pm 0.3$	
5	RB/POM−resin	$\tau_1 = 1.5 \pm 0.1$	$Q_1 = 50$
		$\tau_2 = 5.4 \pm 0.3$	$Q_2 = 50$
6	RB/POM−resin/H_2O_2	$\tau_1 = 0.8 \pm 0.1$	$Q_1 = 57$
		$\tau_2 = 4.8 \pm 0.2$	$Q_2 = 43$

In the RB-only aqueous solution, the decay of the excited dye molecules could be described as single-exponential kinetics ($\tau = 1.5$ ns). Upon addition of POM, which could interact strongly with RB through electrostatic attraction, the fluorescence lifetime of RB seemed to be reduced to a slight extent ($\tau = 1.2$ ns), and this could likely be caused by the electron transfer from the excited RB molecule to POM. Interestingly, when RB was adsorbed on the resin support, its lifetime was prolonged dramatically from 1.5 to 6.0 ns, suggesting that the resin support could stabilize the photoexcited state of the adsorbed RB molecules. However, introduction of H_2O_2 into the RB/resin system had little effect on the lifetime of resin-adsorbed RB (entry 4, Table 2), which further showed that the electron transfer from the photoexcited RB molecule to the oxidant H_2O_2 was unfavorable, and it was consistent with the inefficiency of the photodegradation of RB in the resin/H_2O_2 system. In the RB/POM−resin system, however, the fluorescence decay of RB deviated markedly from the single-exponential kinetics to the double-exponential decay kinetics. The long-lived component ($\tau =$ 5.4 ns) had a lifetime close to that of the resin-adsorbed RB, while the short-lived component ($\tau = 1.5$ ns), most probably, arose from the RB molecules interacting with the resin-supported POMs. In comparison to the above-mentioned binary systems, the complicated interactions between RB, POM, and the resin support seemed to reduce the lifetime of the resin-adsorbed RB molecules and slightly enhance that of the RB molecules interacting with the POM sites on the catalyst. When H_2O_2 was added into the RB/POM−resin system (entry 6, Table 2), the lifetime of the short-lived component was reduced from 1.5 to 0.8 ns, whereas the long-lived component was further reduced from 5.4 to 4.8 ns. Both lifetimes were reduced by addition of H_2O_2, implying that charge transfers from the photoexcited RB molecules to both the POM sites and the resin support of the catalyst were facilitated by H_2O_2. Because we know that H_2O_2 has an oxidative potential of 1.76 V and the reduced POM ($PW_{12}O_{40}^{4-}$) has a negative potential (*5*, *37*), it is reasonable that H_2O_2 could efficiently remove the electrons from the reduced POM under acidic conditions. And it was consistent with the experimental result that RB could be photodegraded efficiently in the POM−resin/H_2O_2 system under visible-light irradiation.

Roles of O_2, H_2O_2, and Related Radicals. By acceptance of an electron from the photoexcited RB molecule, POM can be reduced, and the regeneration of the reduced POM is always a key step in the catalytic cycle. In some reported

cases, O_2 played an important role by accepting an electron from the reduced POM, forming active oxygen species (•OOH and •OH) and restoring the POM to its oxidized form simultaneously (*20*, *41*−*45*). Both inner-sphere and outer-sphere mechanisms have been proposed. According to the inner-sphere mechanism (*41*−*43*), the first step is that the oxidants (O_2, peroxides) interact with the reduced POMs to form covalently bonded M−O intermediates, through which intramolecular electron transfer from the reduced M centers of POMs to the oxidants occurs, then the covalent bond dissociates, forming the reoxidized POM and some active oxygen species; while the outer-sphere mechanism (*44*, *45*) involves no covalent bond between POMs and oxidants, and the electron-transfer process is much faster. It is reported that some Fe^{3+}- or V^{5+}-substituted POMs were more likely to follow the inner-sphere mechanism in which Fe^{3+} or V^{5+} might serve as active centers for coordination with oxidants (*42*, *43*). However, in most advanced oxidation technologies (AOT) for (photo-)catalytic degradation of organic pollutants, the oxidative •OH and •OOH radicals are considered to be predominantly responsible for the degradation of the pollutants (*14*−*16*, *46*−*48*).

To obtain more insight into the roles of O_2 and related •OH and •OOH radicals in the present study, experiments under O_2 and N_2 atmospheres were undertaken, and different radical scavengers for •OH and •OOH radicals were introduced into separate experiments. The results showed that under both O_2 and N_2 (in the absence of O_2) atmospheres degradation of RB exhibited almost the same rate as in an aerated system in the presence of H_2O_2 and POM/resin catalyst under visible-light irradiation, suggesting that the dissolved O_2 played a minor role in the photodegradation of RB in the present system. Isopropyl alcohol, an effective scavenger for •OH radicals, and superoxide dismutase (SOD), an effective scavenger for •OOH radicals, were also introduced into the reaction system in separate experiments to examine the roles of •OH and •OOH radicals. It was found that there was little effect on the degradation rate of RB upon addition of either isopropyl alcohol or SOD into the reaction system, suggesting that the •OH and •OOH radicals were not the dominant active oxygen species involved in the present reaction system. But notably, detailed investigations into the reaction intermediates revealed some differences in these experiments. In the experiments under O_2 atmosphere or upon addition of isopropyl alcohol, the three de-ethylated intermediates of RB as in the aerated system were detected, and they exhibited the same tendency in evolution as those in the aerated system. However, under N_2 atmosphere or upon addition of SOD, neither EER nor DR intermediates could be detected; only the DER, which had a percentage of 5% in the initial solution due to impurities in the raw RB material, was detected and exhibited a quick degradation along with RB in the photoreaction. These results suggested that the formation of de-ethylated intermediates of RB might relate closely to O_2 and •OOH radical. Further investigation into this argument was presented by the detection of •OH and •OOH radicals using spin-trapped EPR measurements.

The EPR signals of the DMPO-trapped •OH radicals in the photodegradation of RB are shown in Figure 6 A. No •OH signals were detected in the dark (bottom spectrum, A), nor was the characteristic signal of •OH observed under the irradiation of a pulsed laser ($\lambda = 532$ nm, 10 Hz) for even 120 s. By sharp contrast, when a trace of Fe^{2+} was introduced into the otherwise identical system without POM/resin catalyst (top spectrum, A), strong signals of the DMPO−•OH adducts emerged even in the dark, in which the •OH radicals were produced by the well-known Fenton reaction (*46*, *47*). Therefore, unlike other AOT systems, it is unreasonable to attribute the degradation of the dye in the present system to the attack of the substrates by •OH radicals, because the

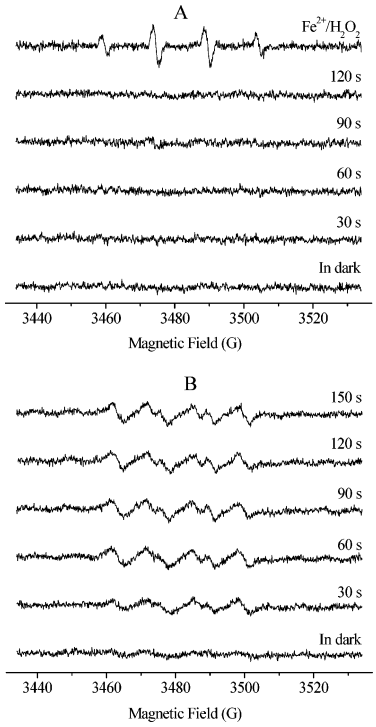

FIGURE 6. EPR signals of (A) DMPO−•OH adducts and (B) DMPO−•OOH adducts for the RB/POM−resin/H_2O_2 system in aerated dispersions in dark and under visible irradiation ($\lambda = 532$ nm).

EPR measurements directly rule out the participation of •OH radicals in the present system. The role of a much weaker oxidative radical, namely, •OOH, was also examined in methanolic media, due to the facile disproportionation of the superoxide species in water (*49*) that precludes the slow reaction between DMPO and •OOH ($k = 10$ and $6.6 \times 10^3\ M^{-1}\ s^{-1}$, respectively) (*50*). From Figure 6 B, one could see that almost no signals could be detected in the dark, while under visible-light irradiation, a set of DMPO−•OOH signals emerged, and the intensity of the signals tended to grow slowly with irradiation time. EPR measurements of •OH and •OOH radicals were also performed in deaerated RB/POM−resin/H_2O_2 dispersions, but at this time, no signal was detected for both radicals. These EPR measurements revealed that DMPO−•OOH signals could be detected only in the presence of O_2 under visible-light irradiation, suggesting that charge transfer takes place from the photoexcited RB molecule to POM and then from the reduced POM to the dissolved O_2, forming the •OOH radicals. When H_2O_2 was employed instead of O_2 as the oxidant under acidic conditions, although neither •OH nor •OOH radical could be formed, it could also efficiently remove the electron accumulated on the reduced POM, facilitating the charge transfer from the photoexcited RB molecule to POM, as suggested by the above-mentioned fluorescence lifetime analysis.

The kinetic and intermediates studies under various conditions, together with the EPR measurements, tend to suggest that O_2 takes part in the reaction system by accepting electrons from the reduced POMs to form •OOH radicals, which accounts for the de-ethylation of RB, resembling what we have observed in an aerated homogeneous POM solution (*20*), and no •OH radicals are involved in the whole system. However, O_2 has a minor influence on the degradation rate of RB and plays almost no role in the decomposition of the conjugated xanthene structure. Then the quick decomposition of the RB dye in the present system should be attributed to the oxidant H_2O_2.

Discussion of the Possible Pathways. As was reported by Ishii et al. (*33*) and Hill et al. (*40*), the precomplexation of

H_2O_2 and POM in homogeneous solution resulted in both decomposition of the parent POM and oxygen transfer from H_2O_2 to POM, forming the seven-coordinate W−O peroxo species, which was the real active species for *selective oxidation* of organic substrates. It was further confirmed by Server-Carrio and co-workers (*34*) that H_2O_2 could react with lacunary POMs with certain heteroatoms, such as P^{5+}, Si^{4+}, and Ga^{3+}, to form four bidentate peroxo polyhedrons surrounding the vacancy without the complete decomposition of the lacunary structure, which actually accounted for the thermal oxidation of olefins and alcohols. In the present system, the POMs loaded on the resin support exhibited incomplete structure as $PW_{11}O_{39}^{7-}$, as proven by the IR analyses shown in Figure 1, trace c, and the specific lacunary structure of the POM on the resin makes it possible for the complexation of POM with H_2O_2 at the lacunary sites. It is consistent with the experimental results that the catalyst prepared at pH 1.0, under which conditions the structure of POM usually remained intact (*38*), and the catalysts prepared at high pH conditions (pH > 6.0), at which the lacunary structure underwent further decomposition (*37*, *38*), exhibited little activity for activation of H_2O_2, suggesting that the lacunary structure of POM was essential for H_2O_2 activation in the present study. This is further supported by IR measurements of the catalyst (Figure 1, trace d). Upon addition of H_2O_2, the peak at 805 cm^{-1} assigned to the vibration of W−O_e−W split into two peaks at 839 and 789 cm^{-1}, respectively. At the same time, the peak around 1045 cm^{-1}, which is the characteristic band of the P−O vibration of $PW_{11}O_{39}^{7-}$ (*38*), decreased dramatically. However, the characteristic bands of W═O_t and W−O_c−W vibrations changed little in position. This indicated that H_2O_2 could react with the W−O octahedron of POM loaded on the resin, most probably at the edge-sharing oxygen positions and the lacunary positions (*34*) of POM loaded on the resin. The peak emerging at 839 cm^{-1} was considered to be attributed to the υ(O−O) stretching of the peroxo species (*3*, *38*). Furthermore, a broad IR band appeared distinctly around 550 cm^{-1} compared to trace c, and it could be confidently assigned to the $\upsilon_s(W(O_2))$ vibration (*34*).

It is clear from the above IR analyses that the seven-coordinate W−O peroxo species were formed on the resin-loaded POMs upon addition of H_2O_2. And the covalently bonded ($W(O_2)$) species represented an inner-sphere mechanism for the regeneration of reduced POMs in the present study, in which no •OH and •OOH radicals were produced as shown by the EPR measurements in a deaerated dispersion. More importantly, the peroxo species should also be the only active oxygen species that account for the decomposition of RB, most probably through the interaction with the $RB^{+\bullet}$ radicals formed by injecting an electron from photoexcited RB to POMs.

On the basis of the above discussions, the photodegradation process of RB catalyzed by POM/resin catalyst with H_2O_2 under visible-light irradiation can be summarized as follows (eqs 1−4):

$$\text{RB} + \text{POM/resin} \rightarrow [\text{RB}-\text{POM/resin}] \quad (1)$$

$$[\text{RB}-\text{POM/resin}] \xrightarrow{h\upsilon} [\text{RB}^*-\text{POM/resin}] \rightarrow [\text{RB}^{+\bullet}-\text{POM}^-/\text{resin}] \quad (2)$$

$$[\text{RB}^{+\bullet}-\text{POM}^-/\text{resin}] \xrightarrow{O_2,\ H^+} [\text{RB}^{+\bullet}\text{- - -POMOOH/resin}] \rightarrow \text{de-ethylated products} \quad (3)$$

$$[\text{RB}^{+\bullet}-\text{POM}^-/\text{resin}] \xrightarrow{H_2O_2} [\text{RB}^{+\bullet}\text{---}\,O\,(O^-)\,W\,/\,\text{resin}]$$

$$\xrightarrow{H_2O_2 + H^+} \text{degradation products} + \text{POM/resin} \quad (4)$$

The initial step is the preassociation between RB and the POM loaded on the resin, which makes it possible for the electron transfer from RB to POM under visible-light irradiation. As stated above that anionic dyes that are repelled by the negatively charged POMs cannot undergo degradation, this process is an important prerequisite in the present study. Visible-light excitation of RB promotes an electron of the dye to a higher energy level, and then the electron migrates to the lowest unoccupied molecular orbital (LUMO) of the POM, forming the reduced POM and $RB^{+\bullet}$ radical (eq 2), which could be inferred from the fluorescence studies and further supported by the fact that the redox potentials of the POMs (for $PW_{11}O_{39},^{7-}$ no literature value is available yet, but it should be close to that of $PW_{12}O_{40}^{3-}$, +0.15 V vs NHE) are more positive than that of the photoexcited RB (RB*, −1.40 V vs NHE). In the presence of O_2, the reduced POMs are slowly reoxidized and the thus formed •OOH radicals that are detected by EPR measurements, accounting for the stepwise de-ethylation of RB (eq 3). When H_2O_2 is used as an oxidant, it regenerates the resin-supported POMs (mainly $PW_{11}O_{39}^{7-}$) more rapidly under acidic conditions in the present system, via an inner-sphere mechanism by forming the seven-coodinate W−O peroxo species. Moreover, the interaction between the active peroxo species and the $RB^{+\bullet}$ radicals causes the efficient degradation and partial mineralization of the RB dye.

In summary, this paper shows that $PW_{12}O_{40}^{3-}$ can be immobilized on the anionic exchange resin through electrostatic interactions, and the thus formed POM/resin material can efficiently catalyze the degradation and even partial mineralization of cationic dye pollutants in the presence of H_2O_2 under visible-light irradiation. The photoreaction mechanism involves an electron transfer from the excited dye to the POM, forming the reduced POM, which can be reoxidized by both H_2O_2 and O_2, and an active peroxo species is generated by the interaction of the POM on the resin with H_2O_2, then the subsequent reaction of the active peroxo species with the dye radicals causes the decomposition of the dye pollutants. The resin-supported POM catalyst is readily separable and reusable without obvious loss of activity. The present study provides a way to utilize visible light in remediation of organic pollutants using POMs.

Acknowledgments

Generous financial support by the Ministry of Science and Technology of China (Grant No. 2003CB415006), the National Science Foundation of China (Grant Nos. 20371048, 20407016, 20537010, 20520120221, 50221201, and 50436040), and the Chinese Academy of Sciences are gratefully acknowledged.

Literature Cited

(1) Hill, C. Introduction: Polyoxometalates—Multicomponent molecular vehicles to probe fundamental issues and practical problems. *Chem. Rev.* **1998**, *98*, 1−2.

(2) Pope, M.; Muller, A. Polyoxometalate chemistry: An old field with new dimensions in several disciplines. *Angew. Chem., Int. Ed. Engl.* **1991**, *30*, 34−48.

(3) Xi, Z.; Zhou, N.; Sun, Y.; Li, K. Reaction-controlled phase-transfer catalysis for propylene epoxidation to propylene oxide. *Science.* **2001**, *292*, 1139−1141.

(4) (a) Kamata, K.; Yonehara, K.; Sumida, Y.; Yamaguchi, K.; Hikichi, S.; Mizuno, N. Efficient epoxidation of olefins with ≥99% selectivity and use of hydrogen peroxide. *Science.* **2003**, *300*, 964−966. (b) Mizuno, N.; Nozaki, C.; Kiyoto, I.; Misono, M. Highly efficient utilization of hydrogen peroxide for selective oxygenation of alkanes catalyzed by diiron-substituted polyoxometalate precursor. *J. Am. Chem. Soc.* **1998**, *120*, 9267−9272.

(5) Hiskia, A.; Mylonas, A.; Papaconstantinou, E. Comparison of the photoredox properties of polyoxometalates and semiconducting particles. *Chem. Soc. Rev.* **2001**, 30, 62−69.

(6) Chambers, R.; Hill, C. Comparative study of polyoxometalates and semiconductor metal oxides as catalysts. Photochemical oxidative degradation of thioethers. *Inorg. Chem.* **1991**, *30*, 2776−2781.

(7) Androulaki, E.; Hiskia, A.; Dimotikali, D.; Minero, C.; Calza, P.; Pelizzetti, E.; Papaconstantinou, E. Light induced elimination of mono- and polychlorinated phenols from aqueous solutions by $PW_{12}O_{40}^{3-}$. The case of 2,4,6-trichlorophenol. *Environ. Sci. Technol.* **2000**, *34*, 2024−2028.

(8) Ozer, R.; Ferry, J. Photocatalytic oxidation of aqueous 1,2-dichlorobenzene by polyoxometalates supported on the NaY zeolite. *J. Phys. Chem. B.* **2002**, *106*, 4336−4342.

(9) Yue, B.; Zhou, Y.; Xu, J.; Wu, Z.; Zhang, X.; Zou, Y.; Jin, S. Photocatalytic degradation of aqueous 4-chlorophenol by silica-immobilized polyoxometalates. *Environ. Sci. Technol.* **2002**, *36*, 1325−1329.

(10) Yoon, M.; Chang, J.; Kim, Y.; Choi, J.; Kim, K.; Lee, S. Heteropoly acid-incorporated TiO_2 colloids as novel photocatalytic systems resembling the photosynthetic reaction center. *J. Phys. Chem. B.* **2001**, *105*, 2539−2545.

(11) Troupis, A.; Hiskia, A.; Papaconstantinou, E. Photocatalytic reduction and recovery of copper by polyoxometalates. *Environ. Sci. Technol.* **2002**, *36*, 5355−5362.

(12) Troupis, A.; Hiskia, A.; Papaconstantinou, E. Synthesis of metal nanoparticles by using polyoxometalates as photocatalysts and stabilizers. *Angew. Chem., Int. Ed.* **2002**, *41*, 1911−1914.

(13) Mandal, S.; Selvakannan, P.; Pasricha, R.; Sastry, M. Keggin ions as UV-switchable reducing agents in the synthesis of Au core−Ag shell nanoparticles. *J. Am. Chem. Soc.* **2003**, *125*, 8440−8441.

(14) Zhang, F.; Zhao, J.; Shen, T.; Hidaka, H.; Pelizzetti, E.; Serpone, N. TiO_2-assisted photodegradation of dye pollutants II. Adsorption and degradation kinetics of eosin in TiO_2 dispersions under visible light irradiation. *Appl. Catal., B* **1998**, *15*, 147−156.

(15) Liu, G.; Li, X.; Zhao, J.; Hidaka, H.; Serpone, N. Photooxidation pathway of sulforhodamine-B. Dependence on the adsorption mode on TiO_2 exposed to visible light irradiation. *Environ. Sci. Technol.* **2000**, *34*, 3982−3990.

(16) Zhao, W.; Chen, C.; Li, X.; Zhao, J.; Hidaka, H.; Serpone, N. Photodegradation of sulforhodamine-B dye in platinized titania dispersions under visible light irradiation: Influence of platinum as a functional cocatalyst. *J. Phys. Chem. B* **2002**, *106*, 5022−5028.

(17) Bianco Prevot, A.; Baiocchi, C.; Brussino, M.; Pramauro, E.; Savarino, P.; Augugliaro, V.; Marci, G.; Palmisano, L. Photocatalytic degradation of Acid Blue 80 in aqueous solutions containing TiO_2 suspensions. *Environ. Sci. Technol.* **2001**, *35*, 971−976.

(18) Le Magueres, P.; Hubig, S.; Lindeman, S.; Veya, P.; Kochi, J. Novel charge-transfer materials via cocrystallization of planar aromatic donors and spherical polyoxometalate acceptors. *J. Am. Chem. Soc.* **2000**, *122*, 10073−10082.

(19) Keys, T.; Gicquel, E.; Guerin, L.; Forster, R.; Hultgren, V.; Bond, A.; Wedd, A. Photophysical and novel charge-transfer properties of adducts between $[Ru^{II}(bpy)_3]^{2+}$ and $[S_2Mo_{18}O_{62}]^{4-}$. *Inorg. Chem.* **2003**, *42*, 7897−7905.

(20) Chen, C.; Zhao, W.; Lei, P.; Zhao, J.; Serpone, N. Photosensitized degradation of dyes in polyoxometalate solutions versus TiO_2 dispersions under visible-light irradiation: Mechanistic implications. *Chem.—Eur. J.* **2004**, *10*, 1956−1965.

(21) Izumi, Y.; Urabe, K. Catalysis of heteropoly acids entrapped in activated carbon. *Chem. Lett.* **1981**, 663−666.

(22) Fujibayashi, S.; Nakayama, K.; Nishiyama, Y.; Ishii, Y. Oxidation of phenols and hydroquinones by dioxygen catalyzed by mixed addenda heteropolyoxometalate on active carbon (NPV_6Mo_6). *Chem. Lett.* **1994**, 1345−1348.

(23) Neumann, R.; Levin, M. Selective aerobic oxidative dehydrogenation of alcohols and amines catalyzed by a supported molybdenum−vanadium heteropolyanion salt $Na_5PMo_2V_2O_{40}$. *J. Org. Chem.* **1991**, *56*, 5707−5710.

(24) Gall, R.; Hill, C.; Walker, J. Carbon powder and fiber-supported polyoxometalate catalytic materials. Preparation, characterization, and catalytic oxidation of dialkyl sulfide as mustard (HD) analogues. *Chem. Mater.* **1996**, *8*, 2523−2527.

(25) Choi, H.; Chang, Y.; Kwon, Y.; Han, O. Incorporation of decavanadate ions into silica gels and mesostructured silica walls. *Chem. Mater.* **2003**, *15*, 3261−3267.

(26) Chen, C.; Lei, P.; Ji, H.; Ma, W.; Zhao, J. Photocatalysis by titanium dioxide and polyoxometalate/TiO_2 cocatalysts. Intermediates and mechanistic study. *Environ. Sci. Technol.* **2004**, *38*, 329−337.

(27) Guo, Y.; Wang, Y.; Hu, C.; Wang, E.; Zhou, Y.; Feng, S. Microporous polyoxometalates POM/SiO_2: Synthesis and photocatalytic degradation of aqueous organocholorine pesticides. *Chem. Mater.* **2000**, *12*, 3501−3508.

(28) Hu, C.; He, Q.; Zhang, Y.; Liu, Y.; Zhang, Y.; Tang, T.; Zhang, J.; Wang, E. Synthesis of new types of polyoxometalate pillared anionic clays: ^{31}P and ^{27}Al MAS NMR study of the orientation of intercalated $PW_{11}VO_{40}^{4-}$. *Chem. Commun.* **1996**, *2*, 121−122.

(29) Friesen, D.; Headley, J.; Langford, C. The photooxidative degradation of *N*-methylpyrrolidinone in the presence of Cs_3-$PW_{12}O_{40}$ and TiO_2 colloid photocatalysts. *Environ. Sci. Technol.* **1999**, *33*, 3193−3198.

(30) (a) Vasylyev, M.; Neumann, R. New heterogeneous polyoxometalate based mesoporous catalysts for hydrogen peroxide mediated oxidation reactions. *J. Am. Chem. Soc.* **2004**, *126*, 884−890. (b) Plault, L.; Hauseler, A.; Nlate, S.; Astruc, D.; Ruiz, J.; Gatard, S.; Neumann, R. Synthesis of dendritic polyoxometalate complexes assembled by ionic bonding and their function as recoverable and reusable oxidation catalysts. *Angew. Chem., Int. Ed.* **2004**, *43*, 2924−2928.

(31) Okun, N.; Anderson, T.; Hill, C. $[(Fe^{III}(OH_2)_2)_3(A\text{−}r\text{-}PW_9O_{34})_2]^{9-}$ on cationic silica nanoparticles, A new type of material and efficient heterogeneous catalyst for aerobic oxidations. *J. Am. Chem. Soc.* **2003**, *125*, 3194−3195.

(32) Kim, S.; Park, H.; Choi, W. Comparative study of homogeneous and heterogeneous photocatalytic redox reactions: $PW_{12}O_{40}^{3-}$ vs TiO_2. *J. Phys. Chem. B* **2004**, *108*, 6402−6411.

(33) Ishii, Y.; Yamawaki, K.; Ura, T.; Yamada, H.; Yoshida, T.; Ogawa, H. Hydrogen peroxide oxidation catalyzed by heteropoly acids combined with cetylpyridinium chloride. Epoxidation of olefins and allylic alcohols, ketonization of alcohols and diols, and oxidative cleavage of 1,2-diols and olefins. *J. Org. Chem.* **1988**, *53*, 3587−3593.

(34) Server-Carrio, J.; Bas-Serra, J.; Gonzalez-Nunez, M.; Garcia-Gastaldi, A.; Jameson, G.; Baker, L.; Acerete, R. Synthesis, characterization, and catalysis of β_3-$[(Co^{II}O_4)W_{11}O_{31}(O_2)_4]^{,10-}$ the first Keggin-based true heteropoly dioxygen (peroxo) anion. Spectroscopic (ESR, IR) evidence for the formation of superoxo polytungstates. *J. Am. Chem. Soc.* **1999**, *121*, 977−984.

(35) (a) Neumann, R.; Gara, M. Highly active manganese-containing polyoxometalate as catalyst for epoxidation of alkenes with hydrogen peroxide. *J. Am. Chem. Soc.* **1994**, *116*, 5509−5510. (b) Neumann, R.; Gara, M. The manganese-containing polyoxometalate, $[WZnMn^{II}_2(ZnW_9O_{34})_2]^{,12-}$ as a remarkably effective catalyst for hydrogen peroxide mediated oxidations. *J. Am. Chem. Soc.* **1995**, *117*, 5066−5074.

(36) Gould, D.; Griffith, W.; Spiro, M. Polyoxometalate catalysis of dye bleaching by hydrogen peroxide. *J. Mol. Catal. A: Chem.* **2001**, *175*, 289−291.

(37) Kozhevnikov, I. *Catalysis by Polyoxometalates*; John Wiley and Sons: New York, 2002.

(38) Pope, M. *Heteropoly and Isopoly Oxometalates*; Springer: Berlin, 1983.

(39) Rocchiccioli-Deltcheff, C.; Fournier, M.; Franck, R.; Thouvenot, R. Vibrational investigations of polyoxometalates. 2. Evidence for anion−anion interactions in molybdenum(VI) and tungsten(VI) compounds related to the Keggin structure. *Inorg. Chem.* **1983**, *22*, 207−216.

(40) Duncan, D. C.; Chambers, R. C.; Hecht, E.; Hill, C. L. Mechanism and dynamics in the $H_3[PW_{12}O_{40}]$-catalyzed selective epoxidation of terminal olefins by H_2O_2. Formation, reactivity, and stability of $\{PO_4[WO(O_2)_2]_4\}^{3-}$. *J. Am. Chem. Soc.* **1995**, *117*, 681−691.

(41) Hiskia, A.; Papaconstantinou, E. Photocatalytic oxidation of organic compounds by polyoxometalates of molybdenum and tungsten. Catalyst regeneration by dioxygen. *Inorg. Chem.* **1992**, *31*, 163−167.

(42) Neumann, R.; Levin, M. Aerobic oxidative dehydrogenation catalyzed by the mixed-addenda heteropolyanion $PV_2Mo_{10}O_{40}^{5-}$: A kinetic and mechanistic study. *J. Am. Chem. Soc.* **1992**, *114*, 7278−7286.

(43) Toth, J.; Melton, J.; Cabelli, D.; Bielski, B.; Anson, F. Electrochemistry and redox chemistry of $H_2OFe^{III}SiW_{11}O_{39}^{5-}$ and OH in the presence of H_2O_2. *Inorg. Chem.* **1990**, *29*, 1952−1957.

(44) Gall, R.; Faraj, M.; Hill, C. Role of water in polyoxometalate-catalyzed oxidations in nonaqueous media. Scope, kinetics, and mechanism of oxidation of thioether mustard (HD) analogs by *tert*-butyl hydroperoxide catalyzed by $H_5PV_2Mo_{10}O_{40}$. *Inorg. Chem.* **1994**, *33*, 5015−5021.

(45) Duncan, D.; Hill, C. Mechanism of reaction of reduced polyoxometalates with O_2 evaluated by ^{17}O NMR. *J. Am. Chem. Soc.* **1997**, *119*, 243−244.

(46) Herrera, F.; Kiwi, J.; Lopez, A.; Nadtochenko, V. Photochemical decoloration of remazol Brilliant Blue and Uniblue A in the presence of Fe^{3+} and H_2O_2. *Environ. Sci. Technol.* **1999**, *33*, 3145−3151.
(47) He, J.; Ma, W.; He, J.; Zhao, J.; Yu, J. Photooxidation of azo dye in aqueous dispersion of H_2O_2/α-FeOOH. *Appl. Catal. B: Environ.* **2002**, *39*, 211−220.
(48) Horikoshi, S.; Hidaka, H.; Serpone, N. Environmental remediation by an integrated microwave/UV-illumination method. 1. Microwave-assisted degradation of rhodamine-B dye in aqueous TiO_2 dispersions. *Environ. Sci. Technol.* **2002**, *36*, 1357−1366.
(49) Sawyer, D.; Valentine, J. How super is superoxide? *Acc. Chem. Res.* **1981**, *14*, 393−400.
(50) Finkelstein, E.; Rosen, G. Rauckman, E. Spin trapping. Kinetics of the reaction of superoxide and hydroxyl radicals with nitrones. *J. Am. Chem. Soc.* **1980**, *102*, 4994−4999.

Received for review February 16, 2005. Revised manuscript received July 1, 2005. Accepted August 19, 2005.

ES050321G